American Journal of Mechanical Engineering and Automation
2018; 5(1): 1-8
http://www.openscienceonline.com/journal/ajmea
ISSN: 2381-6198 (Print); ISSN: 2381-6201 (Online)

INS/GPS Tightly-Coupled Navigation Algorithm Using the Extended Kalman Filter for Crab-Cultivating Ship

Xueyan Sun, Tianhong Pan*, Mian Khuram Ahsan

Department of Automation, Jiangsu University, Zhenjiang, China

Email address

thpan@ujs.edu.cn (Tianhong Pan)
*Corresponding author

To cite this article

Xueyan Sun, Tianhong Pan, Mian Khuram Ahsan. INS/GPS Tightly-Coupled Navigation Algorithm Using the Extended Kalman Filter for Crab-Cultivating Ship. *American Journal of Mechanical Engineering and Automation.* Vol. 5, No. 1, 2018, pp. 1-8.

Received: February 19 2018; **Accepted**: March 15, 2018; **Published**: May 18, 2018

Abstract

The moving area of the crab-farming ship is small. Using the GPS satellite navigation or the INS inertial navigation system separately cannot satisfy the requirement of the positioning accuracy. To overcome this issue, an INS/GPS tightly-coupled navigation is proposed in this paper, which takes the satellite's pseudo-range and pseudo-range-rate as observed variables. To regulate its trajectory, the mathematical model of the tightly-coupled system is established according to the current attitude information of the aquaculture ship. The data is fused by using the extended Kalman filter algorithm, and the navigation accuracy is improved. Compared with the traditional INS/GPS loosely-coupled module, the proposed algorithm achieves a high positioning accuracy and meets the designed requirements.

Keywords

Crab Farming, Navigation, GPS/INS Tightly-Coupled, Extended Kalman Filter

1. Introduction

The meat of river-crab meat is with high-nutritional value (for example, Vitamin A) and becomes a favorite food in China. River crab cultivation has particular and strict requirements for the natural environment in which crabs are farmed, it is, therefore, necessary to pay close attention to the real-time water quality in the aquaculture area. At the same time, to ensure the yield of the river-crab population and to reduce the wastage of feed, it is necessary to lay crab fodder evenly in the aquaculture area. Although China's river-crab farming has achieved industrial-scale operations, it typically relies primarily on manual operation, which is not only inefficient but also extremely costly. For these reasons, the automation of river crab cultivation is a significant trend [1, 2].

To preserve the ecological environment, most river crab farming operations in China adopt the pond model, which results in the operational area of a typical crab-cultivating ship to be quite small. Therefore, the required navigation accuracy that would be necessarily for an unmanned ship is quite high. Due to economic factors, equipping crab farming workships with expensive navigation equipment is impractical. GPS and INS navigation systems provide low-cost solutions, but the use of either system in isolation cannot meet the accuracy requirements of an automated ship. An integrated INS/GPS navigation system is a viable option that can provide higher accuracy than either system in isolation. At a high level, INS/GPS integrated navigation systems have two modes: loosely coupled and tightly coupled.

Loosely coupled modes require independent GPS and INS solutions. Kalman filtering algorithms require that measurement noise is not correlated over time. However, in loosely coupled models the measurement input noise (i.e., the GPS position and velocity) is in fact associated with time, which limits the Kalman filter gain, and measurement update frequency. This, in turn, reduces the accuracy of INS/GPS loosely-coupled integrated navigation [3-7].

For real-time, accurate estimation of a boat's position, velocity, and attitude information, this paper puts forward using a tightly coupled INS/GPS model with the centralized Kalman filter. Firstly, this paper introduces the structure of an unmanned crab-cultivating ship. Secondly, this paper puts forward a mathematical model for a tightly-coupled solution using the extended Kalman filter for INS/GPS navigation data fusion. Finally, an example is provided to illustrate the effectiveness of the proposed method.

2. The System Framework of an Automated Crab-Cultivating Ship

Because the operational area of a river-crab farming ship is small, and because the ship requires operating at a low speed, the chosen model of the ship is a paddle wheeler, as shown in Figure 1. The components of the ship includes: a carrier (paddle wheeler), a control cabinet, a sensor group (monitors water quality parameters like PH, dissolved oxygen, etc); two cameras (observes the water environment); a feeding machine (automatically dispenses crab feed); solar panels, and the left and right paddle wheels (control the movement of the ship) respectively driven by two motors located inside the hull. The integrated navigation device is an integration of the GPS satellite navigation system and INS inertial navigation system, installed on the upper deck directly between the left and right paddle wheels. As the hull of the ship is small, references to position data in this paper should be interpreted as equivalent to the position of the center of mass for the ship at the time of position calculation [8, 9].

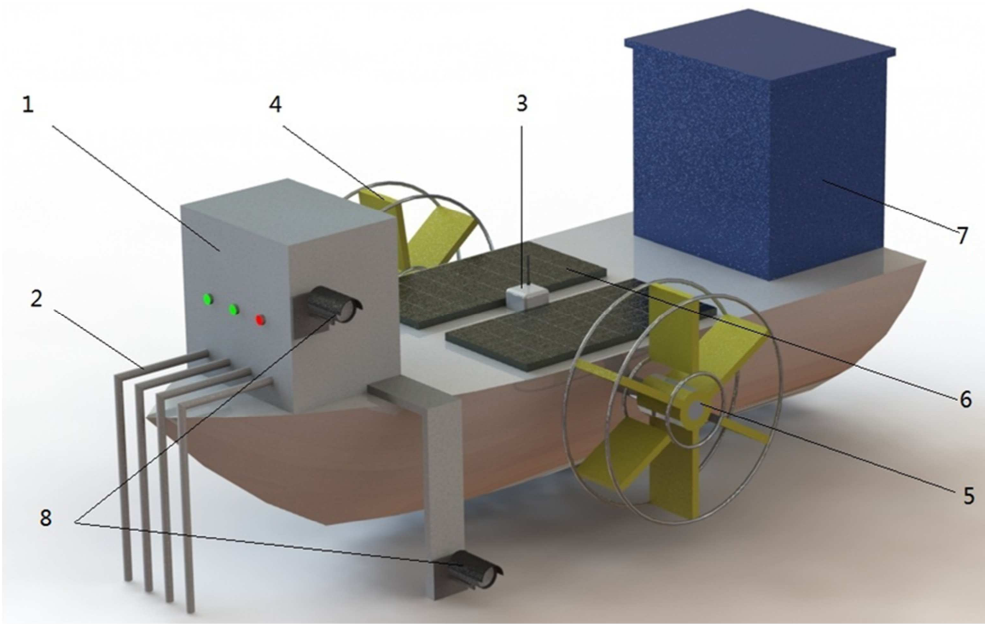

Figure 1. *The structure chart of the crab farming ship.*

1. control cabinet 2. sensor group 3. Integrated navigation device 4. right paddle wheel 5. left paddle wheel 6. solar panels 7. feeding machine 8. cameras

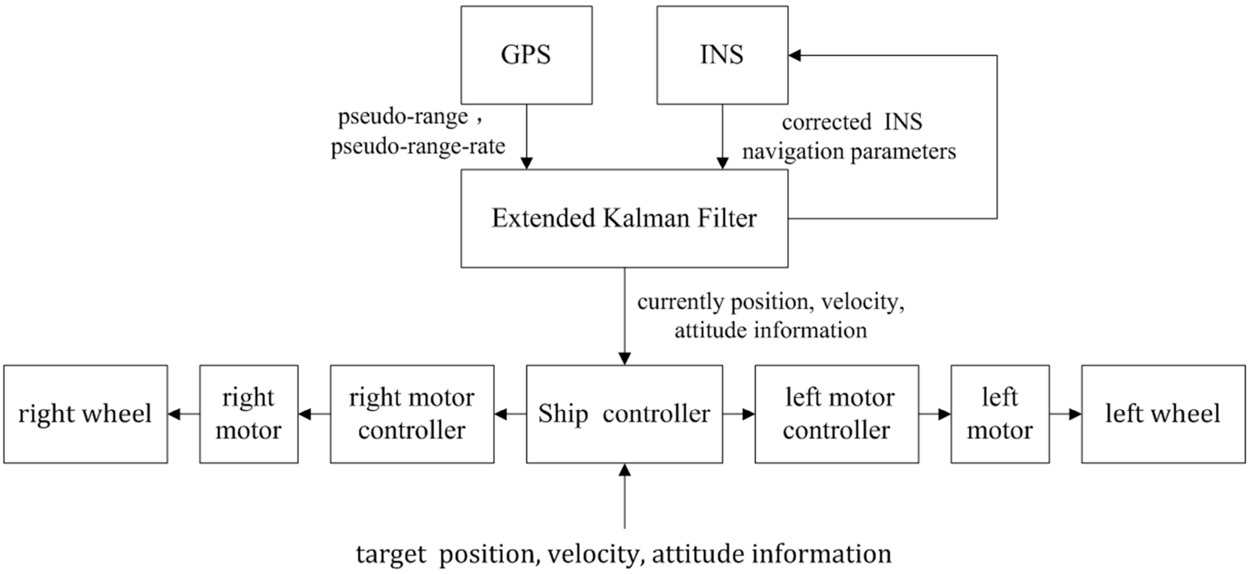

Figure 2. *Crab-cultivating ship navigation system chart.*

The navigation system of the crab-cultivating ship is INS/GPS tightly-coupled navigation, as shown in Figure 2. This system takes the currently satellite's pseudo-range and pseudo-range-rate as observed variables to estimate the INS position error, velocity error, attitude error, GPS clock offset and clock drift. Integrated navigation system model based on inertial navigation equation. Due to the GPS pseudo-range and pseudo-range-rate information has strong non-linear, the extended Kalman filter is used for estimating the INS error, and then use the INS error to correcting the INS navigation parameters. Corrected INS navigation parameters as an output of integrated navigation system and give them to crab-cultivating ship controller. The ship uses the speed of right and left paddle wheels to adjust the ship's navigation state, by comparing the target position, velocity, attitude parameters to the integrated navigation system output.

3. The Mathematical Model of Tightly Coupled System

This paper use Earth-centered Earth-fixed (ECEF) as a reference frame.

3.1. System Model

Based on INS navigation equation, the system model is established. The kinematics equation is:

$$\begin{cases} \delta\dot{\psi}^e_{eb} = -\Omega^e_{ie}\delta\psi^e_{eb} + C^e_b b_g \\ \delta\dot{v}^e_{eb} = f^e_{eb}\psi^e_{eb} + \delta g^e_b(r^e_{eb}) - 2\delta\Omega^e_{eb}v^e_{eb} - 2\Omega^e_{eb}\delta v^e_{eb} \\ \delta\dot{r}^e_{eb} = \delta v^e_{eb} \end{cases} \quad (1)$$

Where: $\delta\psi^e_{eb}$, δv^e_{eb} , δr^e_{eb} are ship's attitude error, velocity error and position error in ECEF, respectively. Ω^e_{ie} is the antisymmetric matrix of angular velocity vector for the earth rotation. This paper is based on the WGS84 gravity model, $\Omega^e_{ie} = 7.292115\times10^{-5}\,rad\cdot s^{-1}$. C^e_b is the coordinate transformation matrix from body frame to ECEF. b_g is Gyro biases, Ω^e_{eb} is the antisymmetric matrix of angular velocity vector by the ship relative to the earth, f^e_{eb} is the specific force measured by the accelerometer, $\delta g^e_b(r^e_{eb})$ is the gravity acceleration error of the navigation ship's position base on WGS84 gravity model.

Clock offset $\delta\rho^a_c$ and clock drift $\delta\dot{\rho}^a_c$ must be estimated because the measurement model of INS/GPS tightly-coupled navigation algorithm adopt GPS receiver to obtain the pseudo-range and pseudo-range-rate as measurement variables.

From the above, the system model of INS/GPS tightly-coupled navigation algorithm at a time is:

$$\dot{x}(t) = F(t)x(t) + G(t)w_s(t) \quad (2)$$

Where: $x = \left(\delta\psi^e_{eb} \quad \delta v^e_{eb} \quad \delta r^e_{eb} \quad b_a \quad b_g \quad \delta\rho^a_c \quad \delta\dot{\rho}^a_c\right)^T$ is state vector, b_a is accelerometer biase, $G(t)$ is the noise distribution matrix of a continuous system, $w_s(t)$ is the white noise of system model.

$$F = \begin{bmatrix} F_I & 0_{15\times2} \\ 0_{2\times15} & F_G \end{bmatrix}, \quad F_I = \begin{pmatrix} -\Omega^e_{ie} & 0_3 & 0_3 & 0_3 & \hat{C}^e_b \\ F^e_{21} & -\Omega^e_{ie} & F^e_{23} & \hat{C}^e_b & 0_3 \\ 0_3 & I_3 & 0_3 & 0_3 & 0_3 \\ 0_3 & 0_3 & 0_3 & 0_3 & 0_3 \\ 0_3 & 0_3 & 0_3 & 0_3 & 0_3 \end{pmatrix}, \quad F_G = \begin{pmatrix} 0 & 0 \\ 1 & 0 \end{pmatrix}$$

$$F^e_{21} = \left[-\left(\hat{C}^e_b \hat{f}^b_{ib}\right)\wedge\right], \quad F^e_{23} = -\frac{2\hat{\gamma}^e_{ib}}{r^e_{eS}(\hat{L}_b)}\frac{\hat{r}^{e\,T}_{eb}}{\left|\hat{r}^e_{eb}\right|}$$

Where: is system matrix, F_I is the system matrix of INS, F_G is the system matrix of GPS's clock offset and clock drift, is a third order identity matrix. Superscript ^ means estimate parameters, $\hat{\gamma}^e_{ib}$ is gravitational acceleration base on the WGS84 model, r^e_{eS} is the distance from ship's position to the earth's core, $\hat{L}_b$ is the latitude where the ship is.

3.2. Measurement Model

The measurement model of Extended Kalman Filter is:

$$z(t) = h\left(x(t), t\right) + w_m(t) \quad (3)$$

Where: $h\left(x(t), t\right)$ is the state vector of a nonlinear system, $w_m(t)$ is the white Gaussian noise with zero mean.

In the INS/GPS tightly-coupled navigation algorithm, the measurement vectors are pseudo-range-rate error and pseudo-range error. The input of the system is:

$$z(t) = \delta z = \begin{pmatrix} \delta z_{\rho,k} \\ \delta z_{r,k} \end{pmatrix} \quad (4)$$

Where:

$$\begin{cases} \delta z_{\rho,k} = (\tilde{\rho}^1_{a,C} - \hat{\rho}^{1-}_{a,C}, \tilde{\rho}^2_{a,C} - \hat{\rho}^{2-}_{a,C}, \cdots \tilde{\rho}^m_{a,C} - \hat{\rho}^{m-}_{a,C})_k \\ \delta z_{r,k} = (\tilde{\dot{\rho}}^1_{a,C} - \hat{\dot{\rho}}^{1-}_{a,C}, \tilde{\dot{\rho}}^2_{a,C} - \hat{\dot{\rho}}^{2-}_{a,C}, \cdots \tilde{\dot{\rho}}^m_{a,C} - \hat{\dot{\rho}}^{m-}_{a,C})_k \end{cases}$$

, $\delta z_{\rho,k}$ is a pseudo-range error, $\delta z_{r,k}$ is a pseudo-range-rate error. $\tilde{\rho}^m_{a,C}$ is the pseudo-range of the satellite-m observed by the receiver of GPS. $\hat{\rho}^{m-}_{a,C}$ is the pseudo-range of the satellite-m, what is calculated from corrected integrated navigation parameters, the estimated clock offset, and clock drift. $\tilde{\dot{\rho}}^m_{a,C}$ is the pseudo-range-rate of the satellite-m observed by the receiver of GPS. $\hat{\dot{\rho}}^{m-}_{a,C}$ is the pseudo-range-rate of the satellite-m, what is calculated from corrected integrated navigation parameters, the estimated clock offset, and clock drift. The subscript k is the number of iterations.

4. Extended Kalman Filter

The steps of extending Kalman filtering algorithm are shown in Figure 3.

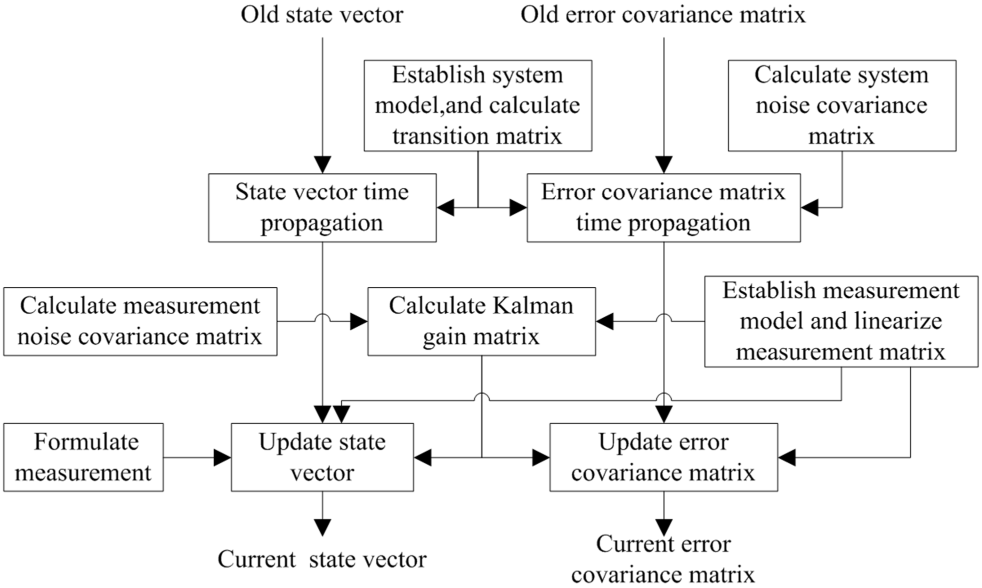

Figure 3. *The steps of extending Kalman filtering algorithm.*

Step 1: Calculate transition matrix

Discretize the system matrix F from the model (2):

$$\Phi \approx \exp(F\tau_s) \tag{4}$$

Where: τ_s is the time between epochs.

The power series is expanded by the time integral, and the first order is:

$$\Phi_I \approx \begin{pmatrix} I_3 - \Omega^e_{ie}\tau_s & 0_3 & 0_3 & 0_3 & \hat{C}^e_b\tau_s \\ F^e_{21}\tau_s & I_3 - 2\Omega^e_{ie}\tau_s & F^e_{23}\tau_s & \hat{C}^e_b\tau_s & 0_3 \\ 0_3 & I_3\tau_s & I_3 & 0_3 & 0_3 \\ 0_3 & 0_3 & 0_3 & I_3 & 0_3 \\ 0_3 & 0_3 & 0_3 & 0_3 & I_3 \end{pmatrix} \tag{5}$$

$$\Phi_G = \begin{pmatrix} 1 & 0 \\ \tau_s & 1 \end{pmatrix} \tag{6}$$

The transition matrix is:

$$\Phi = \begin{bmatrix} \Phi_I & 0_{15\times2} \\ 0_{2\times15} & \Phi_G \end{bmatrix} \tag{7}$$

Step 2: Calculate system noise covariance matrix

The system noise covariance matrix of INS/GPS tightly-coupled navigation algorithm is:

$$Q = \begin{pmatrix} Q_I & 0_{15\times2} \\ 0_{2\times15} & Q_G \end{pmatrix} \tag{8}$$

Due to the short propagation time interval, an approximate matrix can be used.

$$Q_I \approx \begin{pmatrix} S_{rg}I_3 & 0_3 & 0_3 & 0_3 & 0_3 \\ 0_3 & S_{ra}I_3 & 0_3 & 0_3 & 0_3 \\ 0_3 & 0_3 & 0_3 & 0_3 & 0_3 \\ 0_3 & 0_3 & 0_3 & S_{bad}I_3 & 0_3 \\ 0_3 & 0_3 & 0_3 & 0_3 & S_{bgd}I_3 \end{pmatrix}\tau_s \tag{9}$$

$$Q_G = \begin{pmatrix} S_{c\phi}\tau_s & 0 \\ 0 & S_{cf}\tau_s \end{pmatrix} \tag{10}$$

Where: S_{rg} is gyro noise PSD, S_{ra} is accelerometer noise PSD, S_{bad} is accelerometer bias random walk PSD, S_{bgd} is gyro bias random walk PSD. $S_{c\phi}$ is receiver clock phase-drift PSD, conventionally, $S_{c\phi}$ usually take $0.01m^2 \cdot s^{-1}$. S_{cf} is receiver clock frequency-drift PSD. S_{cf} usually take $0.04m^2 \cdot s^{-1}$.

Step 3: State vector time propagation

$$\hat{x}_k^- = \Phi_{k-1}\hat{x}_{k-1}^+ \quad (12)$$

Where: Superscript - means the data before the update, the superscript + means the updated data.

Step 4: Error covariance matrix time propagation

$$P_k^- = \Phi_{k-1}P_{k-1}^+\Phi_{k-1}^T + Q_{k-1} \quad (11)$$

Step 5: Calculate measurement matrix

Linearize measurement model (3):

$$H_k = \left.\frac{\partial h(x(t),t)}{\partial x(t)}\right|_{x=\hat{x}_k^-} = \begin{pmatrix} \dfrac{\partial z_\rho}{\partial \delta\psi_{eb}^e} & 0_{m,3} & \dfrac{\partial z_\rho}{\partial \delta r_{eb}^e} & 0_{m,3} & 0_{m,3} & \dfrac{\partial z_\rho}{\partial \delta\rho_c^a} & 0_{m,1} \\ \dfrac{\partial z_r}{\partial \delta\psi_{eb}^e} & \dfrac{\partial z_r}{\partial \delta v_{eb}^e} & \dfrac{\partial z_r}{\partial \delta r_{eb}^e} & 0_{m,3} & \dfrac{\partial z_\rho}{\partial b_g} & 0_{m,1} & \dfrac{\partial z_r}{\partial \delta\dot{\rho}_c^a} \end{pmatrix}_k \quad (12)$$

The common approximations of analytical solutions for equation (14) are:

$$H_k = \begin{pmatrix} 0_{1,3} & 0_{1,3} & u_{a1}^{e\,T} & 0_{1,3} & 0_{1,3} & 1 & 0 \\ 0_{1,3} & 0_{1,3} & u_{a2}^{e\,T} & 0_{1,3} & 0_{1,3} & 1 & 0 \\ \vdots & \vdots & \vdots & \vdots & \vdots & \vdots & \vdots \\ 0_{1,3} & 0_{1,3} & u_{am}^{e\,T} & 0_{1,3} & 0_{1,3} & 1 & 0 \\ 0_{1,3} & u_{a1}^{e\,T} & 0_{1,3} & 0_{1,3} & 0_{1,3} & 0 & 1 \\ 0_{1,3} & u_{a2}^{e\,T} & 0_{1,3} & 0_{1,3} & 0_{1,3} & 0 & 1 \\ \vdots & \vdots & \vdots & \vdots & \vdots & \vdots & \vdots \\ 0_{1,3} & u_{am}^{e\,T} & 0_{1,3} & 0_{1,3} & 0_{1,3} & 0 & 1 \end{pmatrix}_k \quad (13)$$

Where: u_{am}^e is the unit vector in the direction from the satellite-m to the GPS receiver a, based on ECEF.

Step 6: Calculate measurement noise covariance matrix

The measurement noise covariance matrix in this system is GPS noise covariance matrix. R_g takes the identity matrix in this paper.

Step 7: Calculate Kalman gain matrix

$$K_k = P_k^- H_k^T (H_k P_k^- H_k^T + R_k)^{-1} \quad (14)$$

Step 8: Update state vector

$$\hat{x}_k^+ = \hat{x}_k^- + K_k \delta z_k^- \quad (17)$$

Step 9: Update error covariance matrix

$$P_k^+ = (I - K_k H_k)P_k^- \quad (15)$$

By using Step 1 ~ Step 9, the current state can be estimated from the estimate of the state vector at the previous moment and the measurement vector at present moment.

5. The Experimental Simulation and Analysis

The crab-cultivating ship's navigation system as described in this paper uses the parameters in Table 1.

Table 1. *The design parameters of the crab-cultivating ship.*

Parameters	Numerical value
Length of ship L/mm	1400
Width of ship b/mm	800
Paddle wheels diameter D/mm	400
Maximum speed of paddle wheels R/(r/min)	250
Ship's velocity v/(m/s)	0~5
Throwing radius of feeding machine r/m	5

The location of the ship is equivalent to the installation location of the INS/GPS integrated navigation device, which is close to the center of the rotation axis of the paddle wheels. For experimenting with an area of water measuring $20m \times 40m$, the navigation path shown in Figure 4 is used. The horizontal axis coordinate range is 0~20m, and the vertical axis coordinate range is 0~40m. The area enclosed in this coordinate space is the experimental water area. The navigation path shown in Figure 4 ensures that the ship, equipped with a feeder whose throwing radius is 5m, can project feed over the entire experimental zone. To control the volume of feed delivered into the water area per unit of time, the average navigation speed of Crab-cultivating ship is designed to be 1 m/s. Due to the low speed, the ship maintains this speed of 1 m/s when turning. The coordinate point (5,0) is the starting and ending position, and the navigation direction is clockwise.

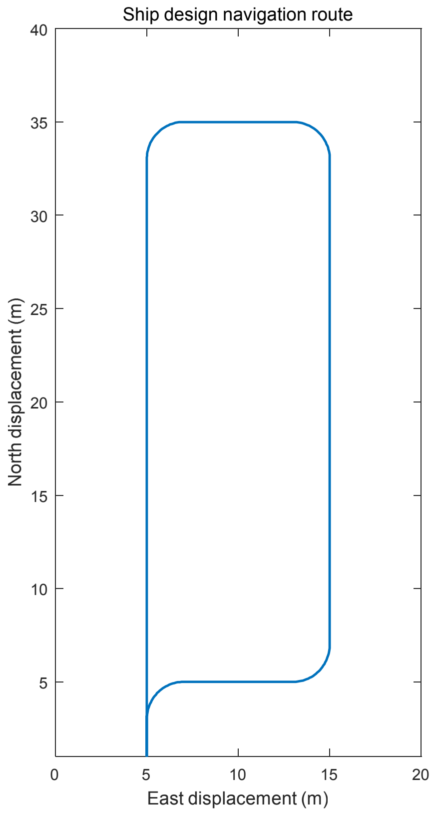

Figure 4. *Ship design navigation route.*

As crab cultivation areas are open and without obstructions, it is assumed there will be no situations where fewer than four GPS satellites are tracked. Therefore, loosely coupled INS/GPS navigation will not diverge as a result of not having enough satellites for GPS positioning. Thus, for this experiment, the comparison of loosely-coupled INS/GPS and tightly-coupled INS/GPS simulations uses the case of positioning with at least four satellites. Both INS/GPS loosely-coupled model and tightly-coupled model use low-end differential GPS system and consumer-class INS equipment.

Figure 5 shows the error curves of INS/GPS loosely-coupled navigation model in a MATLAB environment. Figures 5(a), 5(b) and 5(c) show the ship's North, East, and Down positional error curves in the NED. Figures 5(d), 5(e) and 5(f) show the ship's North, East and Down velocity error curves. Figures 5(g), 5(h) and 5(i) indicate the ship's North, East and Down attitude error curves.

Figure 6 shows the error curves of INS/GPS tightly-coupled INS/GPS navigation model. Figures 6(a), 6(b) and 6(c) show the ship's North, East, and Down positional error curves in the NED. Figures 6(d), 6(e) and 6(f) show the ship's North, East and Down velocity error curves. Figures 6(g), 6(h) and 6(i) show the ships North, East and Down attitude error curves.

Table 2 shows a comparison of the simulation results.

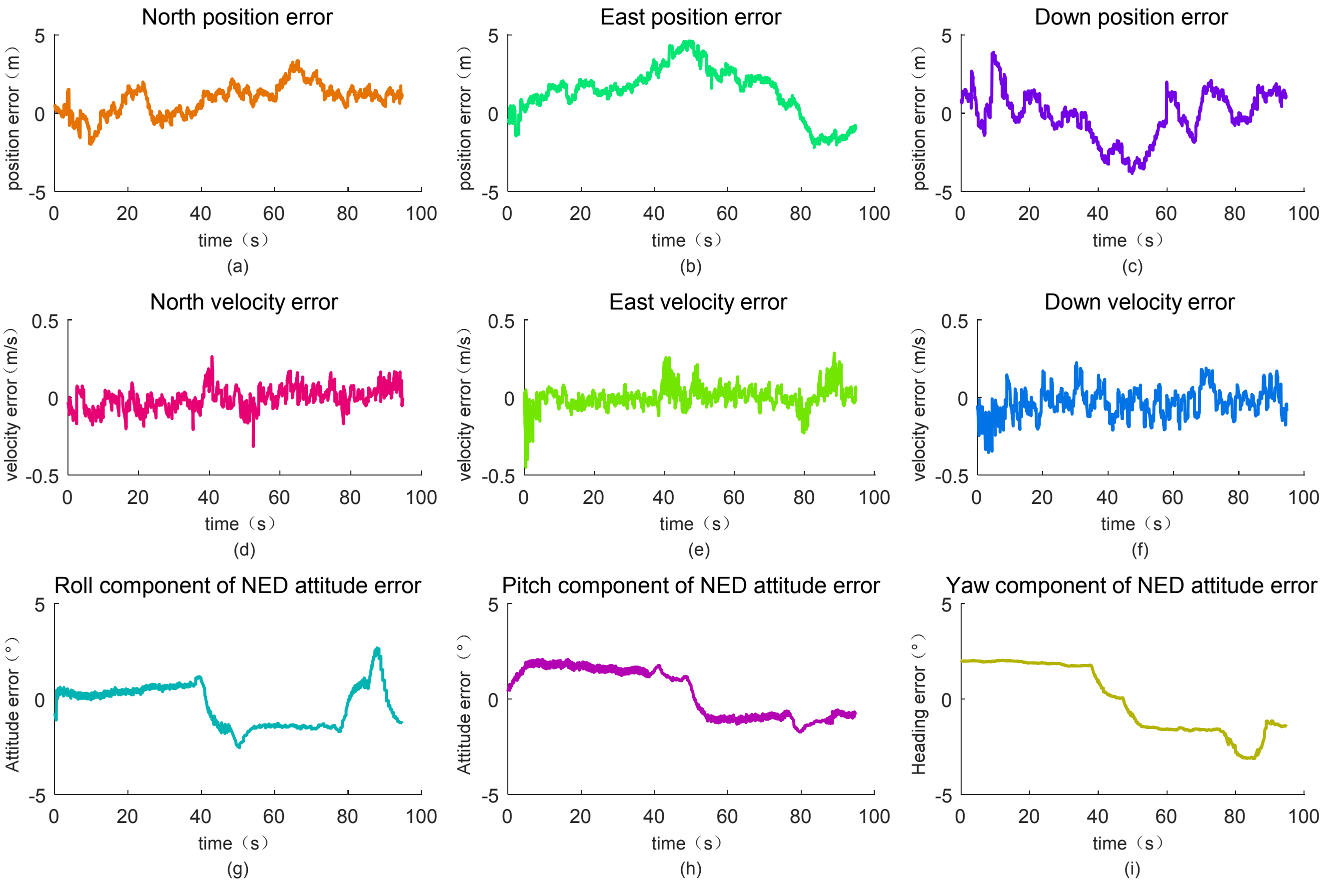

Figure 5. *Loosely-coupled INS/GPS error.*

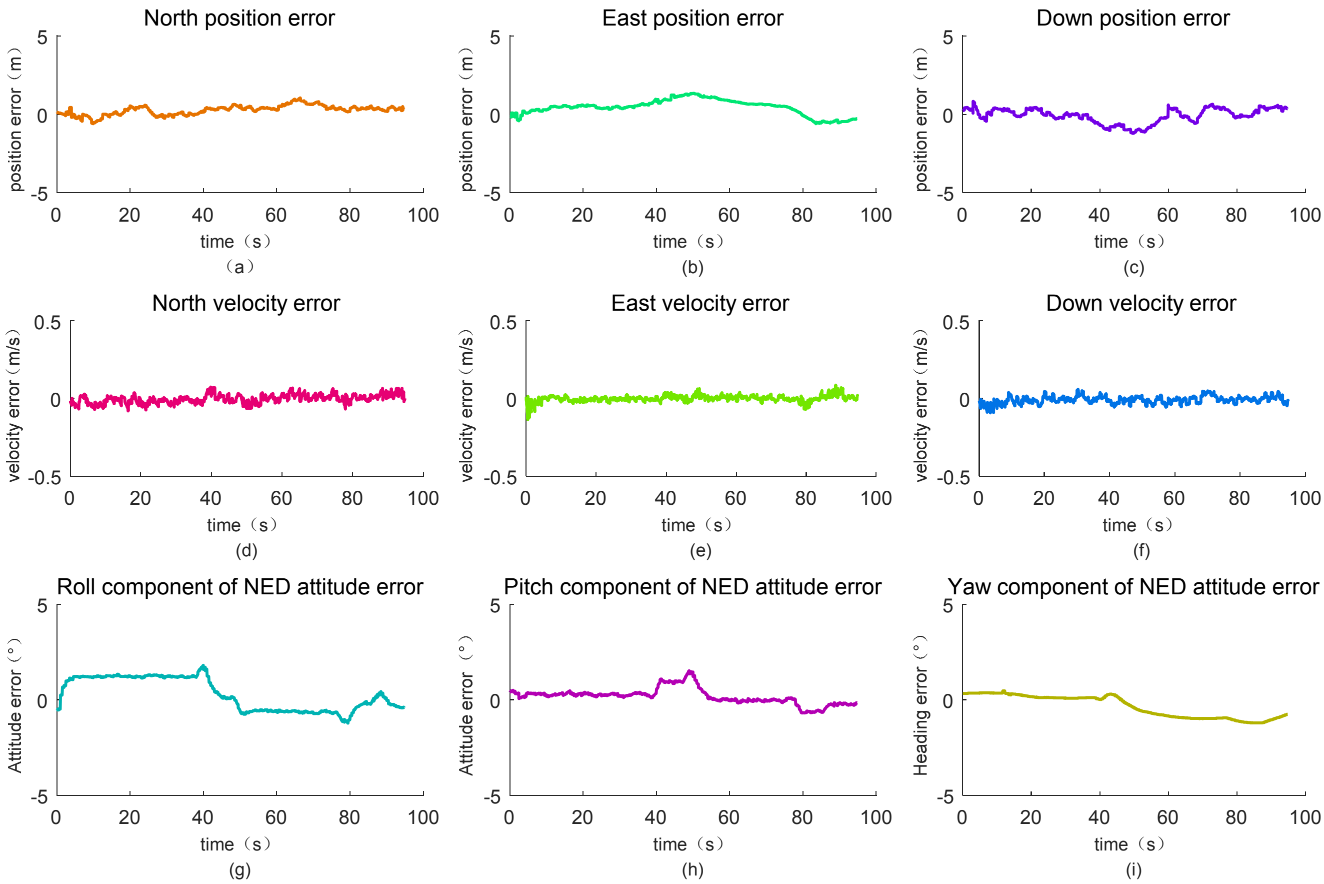

Figure 6. *Tightly-coupled INS/GPS error.*

Table 1. *The precision of INS/GPS loosely and tightly coupled Models Comparison.*

	Loosely-Coupled Model			Tightly-Coupled Model		
	North	East	Down	North	East	Down
Position error δr /m	-2.01~3.35	-2.20~4.60	-3.86~3.87	-0.61~1.04	-0.60~1.33	-1.22~1.22
Velocity error δv /(m/s)	-0.32~0.26	-0.45~0.29	-0.36~0.22	-0.08~0.07	-0.14~0.09	-0.09~0.06
Attitude error $\delta\psi$ /deg	-2.55~2.68	-1.73~2.77	-1.16~1.93	-1.22~1.81	-0.69~1.52	-1.21~0.47

Comparing the error curves in Figure 5 and Figure 6, the tightly coupled INS/GPS position, velocity and attitude error curves are smoother than the loosely coupled error curves under the same conditions. That means the tightly coupled INS/GPS model produces more stable navigation results. At the same time, the data in Table 2 shows that the proposed model has improved accuracy as compared to the INS/GPS loosely-coupled model. The position error, velocity error and attitude error have improved approximately 3 times, 4 times and 2 times respectively. Therefore, under the same conditions, the tightly coupled INS/GPS system has better and more stable navigation accuracy.

6. Conclusion

(1) There is a smoother and more stable error curve between INS/GPS integrated navigation Tightly-coupled model relative to the loosely-coupled model.

(2) In the case of both GPS and INS adopting relatively cheap consumption grade equipment, the accuracy of attitude, velocity, and position in the tightly-coupled model are better than the loosely-coupled model, which reduces the cost of crab farming.

(3) The position error of INS/GPS tightly-coupled Navigation is less than 1.5m, the velocity error is less than 0.15m/s, and the attitude error is less than 2°, which satisfies the precision requirements of the crab-cultivating ship.

References

[1] Zhao D, Luo J, Sun Y, et al. Design and experiment of navigation control system of automatic operation boat in river crab culture [J]. Transactions of the Chinese Society of Agricultural Engineering, 2016, 32 (11): 181-188.

[2] Meng X, Huang J, Xie Q. Online monitoring equipment for aquaculture based on unmanned automatic cruise boat [J]. Transactions of the Chinese Society for Agricultural Machinery, 2015, 46 (3): 276-281.

[3] Zheng X, Fu M. SINS/GPS tightly-coupled integrated navigation [J]. Journal of Chinese Inertial Technology, 2011, 19 (1): 33-37.

[4] Zhou K, Kong J, Zhou X. Analysis on modular navigation ability of coupling GPS/INS [J]. Journal of Chinese Inertial Technology, 2005, 13 (6): 50-53.

[5] Zhou X. The Performance comparison between loose coupling and tight coupling of GPS/INS integrated navigation system [J]." Avionics Technology, 2007, 38 (4): 1-6.

[6] Sun Y, Zhao D, Hong J. Trajectory planning and test for all coverage, automatic and uniform feeding in river crab aquaculture [J]. Transactions of the Chinese Society of Agricultural Engineering, 2016, 32 (18): 190-200.

[7] Gao J, Han H, Bai J. Analysis of Loose Coupling and Tight Coupling of GPS/INS Integrated Navigation System [J]. Journal of Ordnance Equipment Engineering, 2011, 32 (10): 92-96.

[8] Zhao D, Lou J, Sun Y. Design and experiment of navigation control system of automatic operation boat in river crab culture [J]. Transactions of the Chinese Society of Agricultural Engineering, 2016, 32 (11): 181-188.

[9] Liu H, Zhao D, Sun Y. Control system for automatic aquatic plant cleaning ship [J]. Transactions of the Chinese Society of Agricultural Machinery, 2014, 45 (SI): 281-286.

[10] Zhang G, Xu X. Implementation of tightly coupled GPS/INS navigation algorithm on DSP [C]. Computer Design and Applications. IEEE, 2010: 130-134.

[11] Budiyono A. Principles of GNSS, Inertial, and Multisensor Integrated Navigation Systems [J]. Industrial Robot, 2013, 67 (3): 191-192.

[12] Bonnor N. Principles of GNSS, Inertial, and Multisensor Integrated Navigation System-Second Edition Paul D. Groves Artech House [J]. Journal of Navigation, 2014, 67 (1): 191-192.

[13] Li Z, Gao J, Yao Y, et al. GPS/INS tightly-coupled navigation with multipath correction algorithm [J]. Journal of Chinese Inertial Technology, 2014, 22 (6): 782-787.